Hansen, K. A., David, S. V. & Gallant, J. L. Parametric reverse correlation reveals spatial linearity of retinotopic human V1 BOLD response. Neuroimage 23, 233–241

Article *in* NeuroImage · October 2004

Impact Factor: 6.36 · DOI: 10.1016/j.neuroimage.2004.05.012 · Source: PubMed

3 authors, including:

Stephen V David
Oregon Health and Science University
57 PUBLICATIONS **2,444** CITATIONS
SEE PROFILE

Jack Gallant
University of California, Berkeley
75 PUBLICATIONS **6,607** CITATIONS
SEE PROFILE

ELSEVIER

NeuroImage

www.elsevier.com/locate/ynimg
NeuroImage 23 (2004) 233–241

Parametric reverse correlation reveals spatial linearity of retinotopic human V1 BOLD response

Kathleen A. Hansen,[a,b] Stephen V. David,[c] and Jack L. Gallant[a,b,d,*]

[a] *Department of Psychology, University of California, Berkeley, CA 94720-1650, USA*
[b] *Henry H. Wheeler Brain Imaging Center, University of California, Berkeley, CA 94720-1650, USA*
[c] *Program in Bioengineering, University of California, Berkeley, CA 94720-1650, USA*
[d] *Helen Wills Neuroscience Institute, University of California, Berkeley, CA 94720-1650, USA*

Received 30 January 2004; revised 26 April 2004; accepted 7 May 2004

Many experiments measuring blood oxygen level dependent (BOLD) signal in functional magnetic resonance imaging (fMRI) data assume that the BOLD signal is predominantly linear in space and time. Previous investigations of temporal linearity have reported that the temporal BOLD response contains both linear and nonlinear components. Here, we used a novel method to investigate spatial linearity of BOLD within area V1. The visual field was divided into regions shaped like wedges, rings, or the intersections of the wedges and rings. The appearance of a flickering checkerboard texture within each region was governed by an independent M-sequence. fMRI data were acquired as the human subjects maintained visual fixation on a central cross. The time series data from each voxel were cross-correlated with every stimulus sequence to estimate each voxel's BOLD responses to all independent regions of the visual field. Linearity by spatial summation was assessed directly by comparing responses to wedges and rings with sums of responses to component patches. The BOLD responses of voxels responding positively to stimuli, measured with independent stimuli subtending several degrees of visual angle, were well predicted by linear spatial summation.

Keywords: Voxel; Wedge; Ring; M-sequence

Introduction

Many experiments using fMRI assume that the blood oxygen level dependent (BOLD) signal is predominantly linear in space and time. This assumption implies a critical property: the BOLD response to the sum of N stimuli is equal to the sum of the N BOLD responses to the component stimuli (i.e., additivity). The assumption of linearity is particularly convenient because many analytical tools are available for investigating and modeling linear systems. However, the BOLD response is not necessarily linear, in either space or time. Several previous studies have investigated temporal linearity of the BOLD response (Birn et al., 2001; Boynton et al., 1996; Dale and Buckner, 1997; Friston et al., 1998). BOLD responses to stimuli extending over several seconds are well predicted by linear temporal summation, but BOLD responses to brief stimuli are larger than predicted. In this report, we test linearity of spatial summation of BOLD responses within human primary visual cortex (V1).

If linearity by spatial summation holds, then the BOLD response to a stimulus occupying a given expanse of visual space will equal the sum of responses to stimuli occupying component parts of that space:

$$B[1 + \ldots + n] = B[1] + \ldots + B[n] \quad (1)$$

Here, the left side of the equation represents the BOLD response to a stimulus composed of several parts numbered 1 through n, and presented simultaneously; the right side represents the responses to the component stimuli presented independently. If linearity by spatial summation holds, this equation should predict each voxel's responses.

We used a new method of estimating retinotopic selectivity to test this hypothesis directly. To gather data representing the left or right sides of Eq. (1), we conducted three successive fMRI experiments (approximately 13 min each). To minimize spatial stimulus correlations and facilitate linearity analysis, the time course of each stimulus was determined by an M-sequence (Baseler et al., 1994; Buracas and Boynton, 2002; Slotnick et al., 1999; Sutter, 1992). Responses were analyzed using reverse correlation, a form of linear regression. Reverse correlation does not require prior knowledge of the time course of the response (de Boer and Kuyper, 1968; Marmarelis and Marmarelis, 1978). Finally, statistical significance of BOLD responses was estimated by randomization (permutation) tests (Manly, 1991; Mazer et al., 2002).

This combination of procedures enabled us to obtain retinotopic response data objectively, using both whole wedges and rings (left side of Eq. (1)) and their component patches (right side of Eq. (1)). To test linearity by spatial summation, we simply compared the BOLD response of each voxel estimated using

* Corresponding author. Department of Psychology, Helen Wills Neuroscience Institute, University of California, 3210 Tolman #1650, Berkeley, CA, 94720-1650. Fax: +1-510-642-5293.
E-mail address: gallant@socrates.berkeley.edu (J.L. Gallant).
Available online on ScienceDirect (www.sciencedirect.com.)

1053-8119/$ - see front matter © 2004 Elsevier Inc. All rights reserved.
doi:10.1016/j.neuroimage.2004.05.012

whole wedges and rings to the sum of the responses estimated using the component patches. Our findings demonstrate that the retinotopic BOLD responses of voxels responding positively to stimuli and located within V1 are largely consistent with linearity by spatial summation.

Materials and methods

Data acquisition

Imaging was performed on a 4-T INOVA scanner (Varian, Inc., Palo Alto, CA) with a transmit/receive TEM head coil (MR Instruments, Inc., Minneapolis, MN) and a whole-body gradient set capable of 35 mT/m with a rise time of 300 μs (Tesla Engineering, Ltd., Sussex, UK). EPI (two-shot, TR = 0.5 s/half k-space = 1 s; TE = 0.028 s) functional and GEMS (TR = 0.2 s; TE = 0.005 s) in-plane anatomical data were acquired. For both functional and in-plane anatomical data, eight slices approximately parallel to the calcarine sulcus were acquired with thickness 4.14 mm and a gap of 0.5 mm. The functional field of view was 224 × 224 mm and matrix size 64 × 64 pixels; the in-plane anatomical field of view was 224 × 224 mm and matrix size 256 × 256 pixels. A 3D MP-FLASH anatomical data set was also acquired during each functional imaging session. Its central slice was in a plane parallel to the functional slices, and the field of view was 224 × 224 × 198 mm and matrix size 256 × 256 × 128 pixels. We collected data from two subjects (one author) who reported that they maintained fixation and experienced a relatively constant general arousal level throughout the session. Subjects lay supine in the bore of the magnet and viewed the reflected image of stimuli projected onto a backlit translucent screen, fixing their gaze on a central cross. Before the experiment, one subject (SVD) positioned a small occluder that ensured that the real image from the tangent screen was not visible in the visual periphery; the second subject (KNK) did not use an occluder. Ten functional brain volumes (10.0 s) were acquired before beginning stimulus presentation to allow the fMR signal to reach equilibrium. The experimental protocol was approved by the Committee for the Protection of Human Subjects at the University of California, Berkeley.

Stimulus generation and presentation

During functional experiments, the Presentation software package (Version 0.55, www.neurobs.com) controlled stimulus presentation and ensured synchronization between the scanner and the stimuli. All images were precomputed using Matlab (Version 6.0, Mathworks, Inc.) and stored as bitmaps.

Spatial characteristics of stimuli

Three different stimulus sets (Fig. 1) were used in three successive experiments. The wedge set consisted of eight adjacent 45° wedges; the ring set consisted of three concentric rings; and the patch set consisted of 24 patches encompassing the intersections of the wedges and rings. At any point in time, each wedge, ring, or patch was either ON (containing black and white checks that reversed contrast eight times per second) or OFF (isoluminant gray). The background was isoluminant gray at all times. The checks and all ring and patch shapes were scaled with eccentricity according to $S = \cos(Cr^{1/6})$, where S is a 2D matrix representing a concentric circular grating; C is a constant selected such that each wedge, ring or patch contained an integer number of checks; and r is the radius in pixels. S was thresholded to produce maximum contrast. The stimuli covered a maximum of 38° of visual angle (19° radius), but the central 6.0° (3.0° radius) were never used; this parafoveal region had the same luminance as the background. A red central cross (2.0°) was always present and served as a fixation target. The stimuli used here were comparable in size to those used in typical retinotopic mapping and V1 BOLD studies (DeYoe et al., 1996; Engel et al., 1997; Sereno et al., 1995; Tong and Engel, 2001).

Temporal characteristics of stimuli

The temporal sequence of ON and OFF states for each wedge, patch, and ring was an M-sequence. A similar approach has been used to map the retinotopic representation of patch-shaped stimuli using visual evoked potentials (Baseler et al., 1994; Slotnick et al., 1999). A single, 255-bit binary M-sequence was generated from a set of coefficients representing a primitive polynomial with linearly independent roots (Sutter, 1992). A shifted version of this sequence

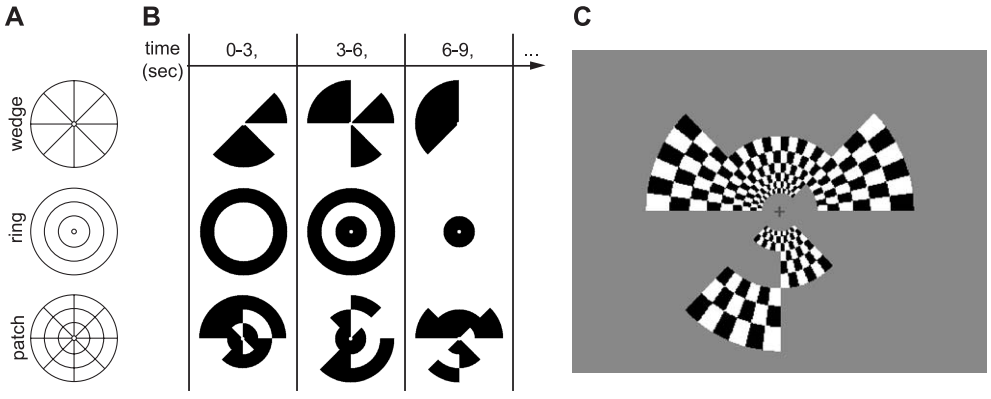

Fig. 1. Spatial and temporal stimulus characteristics. (A) Each grid illustrates regions of the visual field used as stimuli in one of the three (wedge, ring, and patch) experiments. (B) Each row represents schematically the first three ON–OFF states of the binary M-sequences used to control checkerboards in each experiment. Black: ON regions. White: OFF regions and background. Each state lasted 3.0 s. (C) One stimulus frame from the patch experiment (corresponding to panel B, third column), as it appeared to subjects. ON regions contained a black and white checkerboard that reversed contrast eight times per second. OFF regions and background were isoluminant gray.

was assigned to each wedge, patch, and ring. The minimum length of time between a given element in any two versions of the M-sequence was 30 s. Each ON and OFF stimulus state lasted 3 s. The total length of functional data acquisition was 12.75 min × 3 experiments = 38.25 min.

Correlations between a binary M-sequence and shifted versions of the same sequence are vanishingly small. (If the elements of a binary M-sequence are assigned values of −1 or 1, then the autocorrelation at each lag other than zero is equal to $-1/m$, where m is the length of the sequence in bits.) In fact, the autocorrelation of an M-sequence is substantially less than that of random binary sequences (Buracas and Boynton, 2002). By using several shifted versions of an M-sequence to control the ON and OFF states of all stimulus regions in parallel, we ensured that the events in each region were essentially uncorrelated over space and time, thereby preventing artifacts due to stimulus correlations.

Reverse correlation

We used reverse correlation (Marmarelis and Marmarelis, 1978) to estimate retinotopic tuning curves for each voxel. (Reverse correlation and all other data analysis procedures were written in Matlab, Version 6.0, Mathworks, Inc.) Reverse correlation is related to multiple regression, and it is particularly useful when the temporal component of the response is important or unknown (Shmuel et al., 2002). It allows direct estimation of the relationship between the stimulus sequence and the raw time series data, without requiring prior convolution of time series data with some assumed ideal hemodynamic response.

In our reverse correlation procedure, the temporal response function of each voxel, $h(\tau)$, was estimated from the cross-correlation of the fMR time series data, $R(t)$, and the time-offset stimulus sequence, $S(t-\tau)$:

$$h(\tau) = \frac{1}{\sigma_S^2 T}\sum_{t=1}^{T} R(t)(S(t-\tau) - \bar{S}) \quad (2)$$

Here, t denotes a moment in real time, σ_S^2 denotes the variance of the stimulus sequence, T denotes the total number of time points, τ denotes the time lag between the stimulus and a particular component of the hemodynamic response, and $\bar{S}$ denotes the mean value of the stimulus sequence. (Since all stimulus sequences are shifted versions of the same M-sequence, the values of $S(t-\tau)$, σ_S^2, $\bar{S}$, and T are constant across functional runs. $\bar{S}$ was included in our analysis to center the stimulus input values, 0 for OFF and 1 for ON, around a mean of 0. This operation ensured that $h(\tau) = 0$ represents the intuitive case in which a voxel's signal level is uncorrelated with the stimulus sequence.) Each voxel's $h(\tau)$ is its first-order linear temporal kernel. In this paper, we refer to $h(\tau)$ as a voxel's "BOLD response" to a particular wedge, ring, or patch. $h(\tau)$ is in units of raw fMRI signal per unit stimulus, analogous to the unit of neuronal spikes per unit stimulus used to describe reverse correlation results in the electrophysiology literature.

Eq. (2) was applied directly to the reconstructed image data after correcting the data for staggered slice acquisition times. The same slice acquisition timing paradigm was used in all experiments. No normalization between voxels, subjects, or functional runs was performed.

We estimated the BOLD response separately for each analyzed voxel to each wedge, ring, and patch. The set of all responses estimated within the wedge, ring, and patch stimulus classes comprised three complete spatiotemporal tuning curves for each voxel.

Statistical significance

We used randomization (permutation) tests (Manly, 1991) to estimate the statistical significance of the correlation between each voxel's time series data and the shifted M-sequence determining the appearance of each wedge, ring, or patch. For each voxel, the stimulus sequence was shuffled randomly over time and then cross-correlated with the time series data; this shuffling procedure was repeated 500 times. The resulting randomized distribution represented estimated BOLD responses that might be obtained if there were no systematic relationship between the stimulus sequence and the voxel's response properties. The proportion of randomized correlations greater than the observed correlation represents p, the probability that the relationship between that stimulus sequence and the estimated BOLD response was due to chance.

The randomization test is a non-parametric inferential statistic that makes no assumptions about the shape of the data distributions. Conventional parametric statistics assume that the data are distributed normally and that the variances obtained under all conditions are equal. When these assumptions are violated, conventional statistical tests tend to be less powerful than randomization tests (Manly, 1991; Raz et al., 2003).

Selection of voxels

First, we selected all voxels that gave a significant positive BOLD response to at least one of the stimuli in each of the wedge, ring, and patch experiments ($p < 0.05$, corrected for multiple comparisons between stimuli). This test allowed us to avoid including misleading results from voxels in unstimulated cortex (parafovea and far periphery). Our selection process did not require that significant patches be located within significant wedges or rings; the test was applied to each of the three data sets independently. However, we flagged voxels whose patch responses were not located within significant wedges or rings, and analyzed those separately (see Results). Because the statistical significance of each voxel's responses in the experiments of interest governed the selection process, no separate localizer experiment was needed to define a functional region of interest.

The calcarine sulcus was used as an anatomical boundary to exclude non-V1 voxels from our analysis. We identified the calcarine sulcus by inspection of the 3D, high-resolution anatomical data sets, acquired so that every third point along one dimension coincided with one functional slice center (Duvernoy, 1999). After marking the calcarine sulcus on the 3D anatomical data set, we aligned the functional and 3D anatomical data appropriately and identified every functional voxel predominantly representing calcarine gray matter. Although human primary visual cortex sometimes extends beyond the calcarine sulcus, this method reliably restricted the analysis to voxels within area V1.

Results

Our procedure produced many BOLD responses for each calcarine voxel: one for each of the eight wedges, three rings, and 24 patches used in the three functional experiments. ("BOLD response" denotes the response estimated using reverse correlation

between a stimulus sequence and a single voxel's raw time series data, as described in Materials and methods.) Fig. 2C shows the 24 BOLD responses elicited by the patch experiment in a single voxel (location in brain, Figs. 2A/B). Each trace reflects this voxel's response to one of the 24 patches. This voxel gave a significant positive response to three of the patches and a significant negative response to one patch ($p < 0.05$, corrected for multiple comparisons). Responses to the other 20 patches were no different than would be expected by chance. Of the significant positive responses, two reached their peak values 4.0 s after stimulus onset. This was the most commonly observed peak response lag for each subject, and subsequent figures incorporate data at this peak lag only.

At first, it may seem odd that any single V1 voxel can respond positively to several patches, each of which is substantially larger than the receptive field of a typical V1 neuron. However, the voxel referred to in Fig. 2C is located retinotopically between two clusters of voxels, one responding only to the patch shaded red (Fig. 2D) and one responding only to the patch shaded orange (Fig. 2E). Thus, the population of neurons represented by this voxel likely respond to a region of visual space lying on the border between the two patches.

Fig. 3 provides an example of a reverse correlation response set for a ring data set at peak lag (Figs. 3B–D). The grayscale value in each box represents the magnitude or significance of estimated

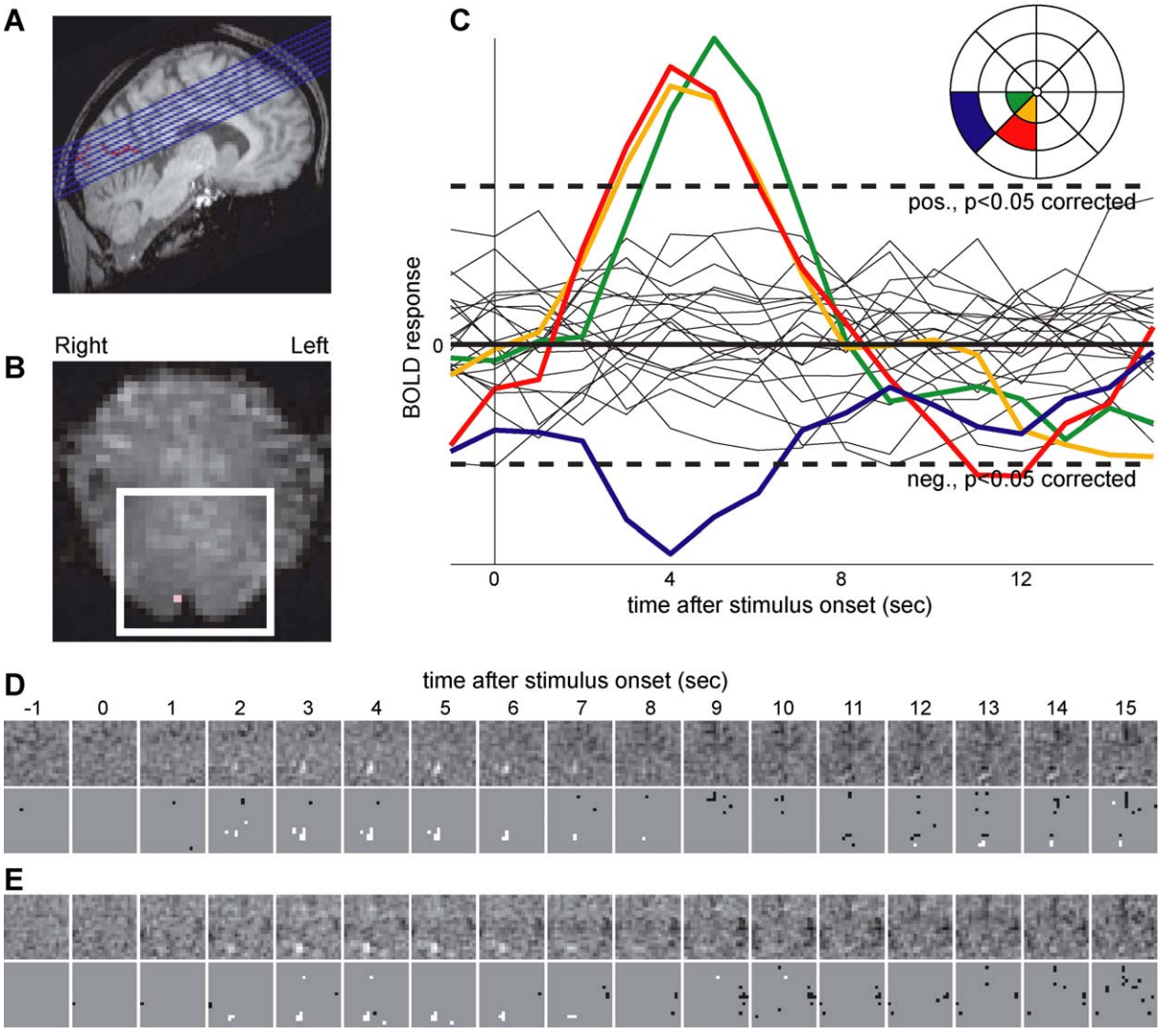

Fig. 2. BOLD responses to patches. (A) 8 functional slices (blue) were acquired approximately parallel to the calcarine sulcus (red). (B) Functional analyses were restricted to a 20 × 20 voxel area of each slice (white box). Functional responses of the voxel shaded pink are shown in panel C. (C) Each of the 24 traces represents the BOLD response of the pink voxel in panel B to a different patch. In this voxel, four patches elicited significant positive or negative responses at the peak lag of 4.0 s (see colored key at upper right; trace color matches patch color). Since V1 is retinotopic, the majority of patches evoked no significant response at peak lag. Units are raw fMRI signal per unit stimulus (Eq. (2), Materials and methods). Values above 0 indicate positive responses; values below 0 indicate negative responses. (D) BOLD responses in multiple voxels elicited by one patch. Each small box shows results from the 20 × 20 square outlined in panel B at a different time lag after stimulus onset. Top row: BOLD responses to the patch shown in red in panel C. Grayscale values are normalized to span the range between highest and lowest BOLD responses to this patch (white = highest; black = lowest). Bottom row: Significance of responses shown in top row (white = positive response, $p < 0.05$, corrected for multiple comparisons; gray = no significant response; black = negative response, $p < 0.05$, corrected for multiple comparisons). (E) BOLD responses in multiple voxels elicited by orange patch in panel C. Format is same as in panel D.

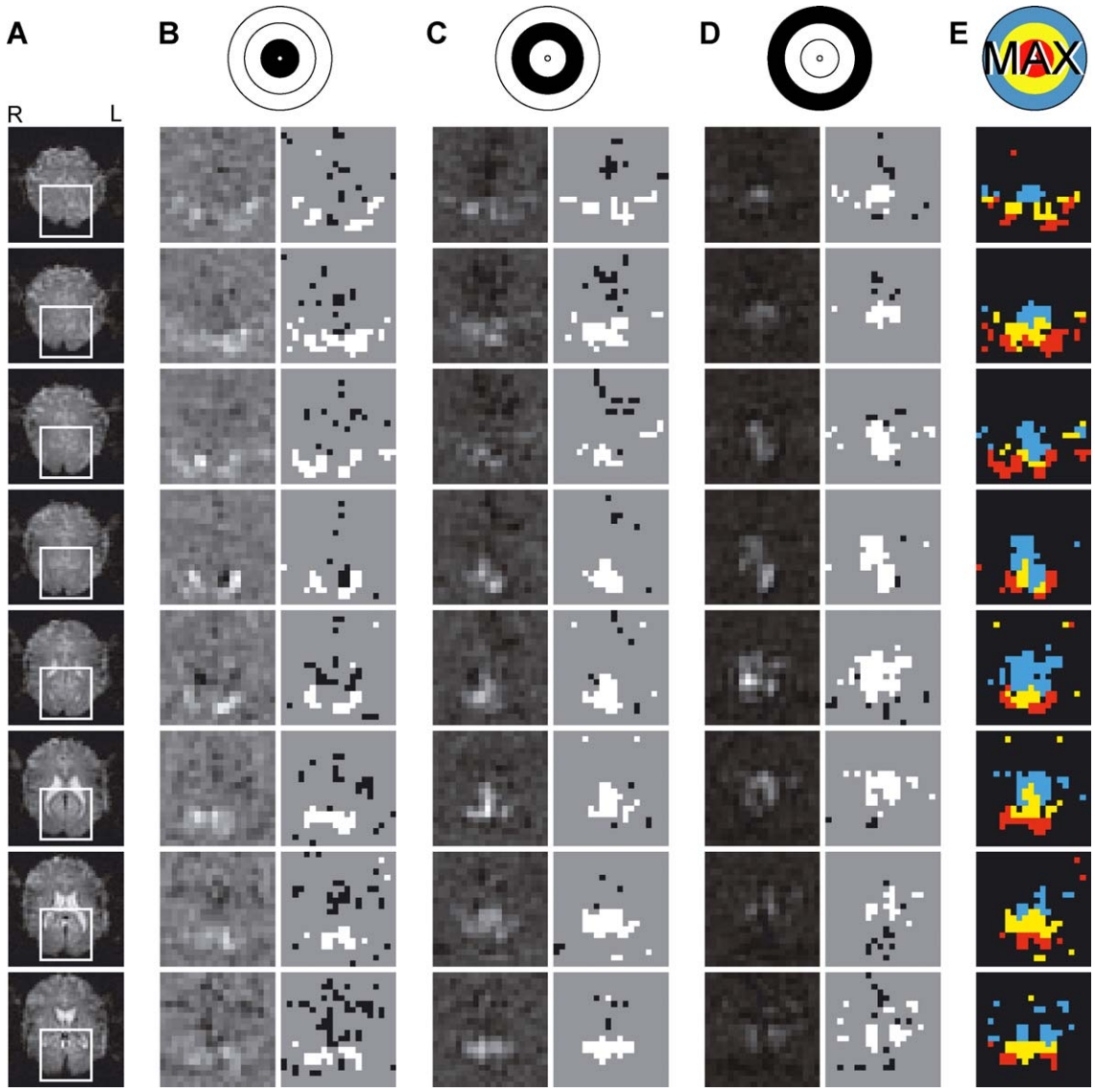

Fig. 3. BOLD responses to ring stimuli at peak lag. (A) Eight slices of one raw functional volume. White boxes indicate analyzed volume (20 × 20 functional voxels per slice). (B) Left column indicates each voxel's BOLD response to the inner ring illustrated at the top. Grayscale values are normalized to span the range between highest and lowest BOLD responses associated with this ring (white = highest; black = lowest). Right column indicates significance of each voxel's BOLD response to the same stimulus (white = positive response, $p < 0.05$, corrected for multiple stimuli; gray = no significant response; black = negative response, $p < 0.05$, corrected for multiple stimuli). (C) BOLD responses to the middle ring (left column) and statistical significance of responses (right column). Format is same as in panel B. (D) BOLD responses to the outer ring (left column) and statistical significance of responses (right column). Format is same as in panel B. (E) The color of each voxel labels the ring associated with that voxel's maximal response. Only voxels responding positively ($p < 0.05$, corrected for multiple comparisons) to at least one ring are labeled.

BOLD responses in one slice: that is, a cross-section across lags of a population of first-order kernels in brain space.

Consistent with previous results (DeYoe et al., 1996; Engel et al., 1997; Sereno et al., 1995; and many other studies), more posterior voxels respond positively to the innermost ring, while anterior voxels tend to respond to more peripheral rings. This pattern can be seen in both the BOLD response *magnitude* obtained by reverse correlation (left column of each pair) and the *statistical significance* of the BOLD response (right column of each pair).

In Fig. 3E, each voxel is color-coded to indicate qualitatively which ring was associated with the maximal response. This representation of the data set provides an intuitive spatial overview of the positive responses, although in many respects it is obviously less informative than the representation in Figs. 3B–D.

Positive BOLD responses are consistent with linearity by spatial summation

Linearity by spatial summation (Fig. 4 and Eq. (1)) predicts that each voxel's response to a wedge or ring will equal the sum of its responses to the component patches. Fig. 5 illustrates the results of a test of this hypothesis for two individual subjects. In each plot, the *y*-axis represents the left side of Eq. (1) (responses to whole wedges or rings), and the *x*-axis represents the right side of Eq. (1) (sums of responses to component patches). Points represent voxels

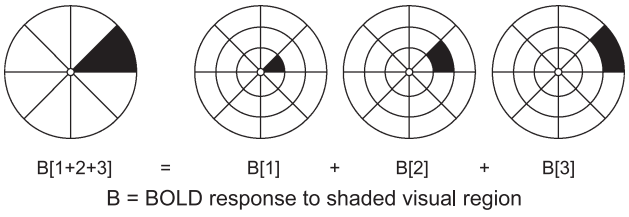

Fig. 4. Schematic of the linear prediction. If a voxel's BOLD response to a given region of visual space (left side of equation) is equal to the sum of the same voxel's BOLD responses to that region's component parts (right side of equation), then that voxel's BOLD response is linear by spatial summation.

responding significantly and positively at peak lag to at least one wedge, at least one ring and at least one patch. For each voxel, the wedge or ring associated with the maximal response was identified. The size of the BOLD response at peak lag to that wedge or ring is plotted on the *y*-axis. The voxel's BOLD responses to all component patches of the same wedge or ring were then summed. The sum is plotted on the *x*-axis.

This representation allows a direct test of Eq. (1) (Fig. 4). If linearity by spatial summation holds, points should fall along the line of unity slope. A suppressive nonlinearity would be revealed if wedge or ring responses were consistently smaller than predicted by patch sums. A facilitatory nonlinearity would be revealed if wedge or ring responses were consistently greater than predicted by patch sums. These data provide clear support for linearity by spatial summation. Most points fall near the line of unity slope. The spread is small (see values of *r*, Fig. 5) and the outliers are distributed symmetrically above and below the line of unity slope.

If every voxel responded to one and only one patch, the above results would be a trivial demonstration of linearity. A more

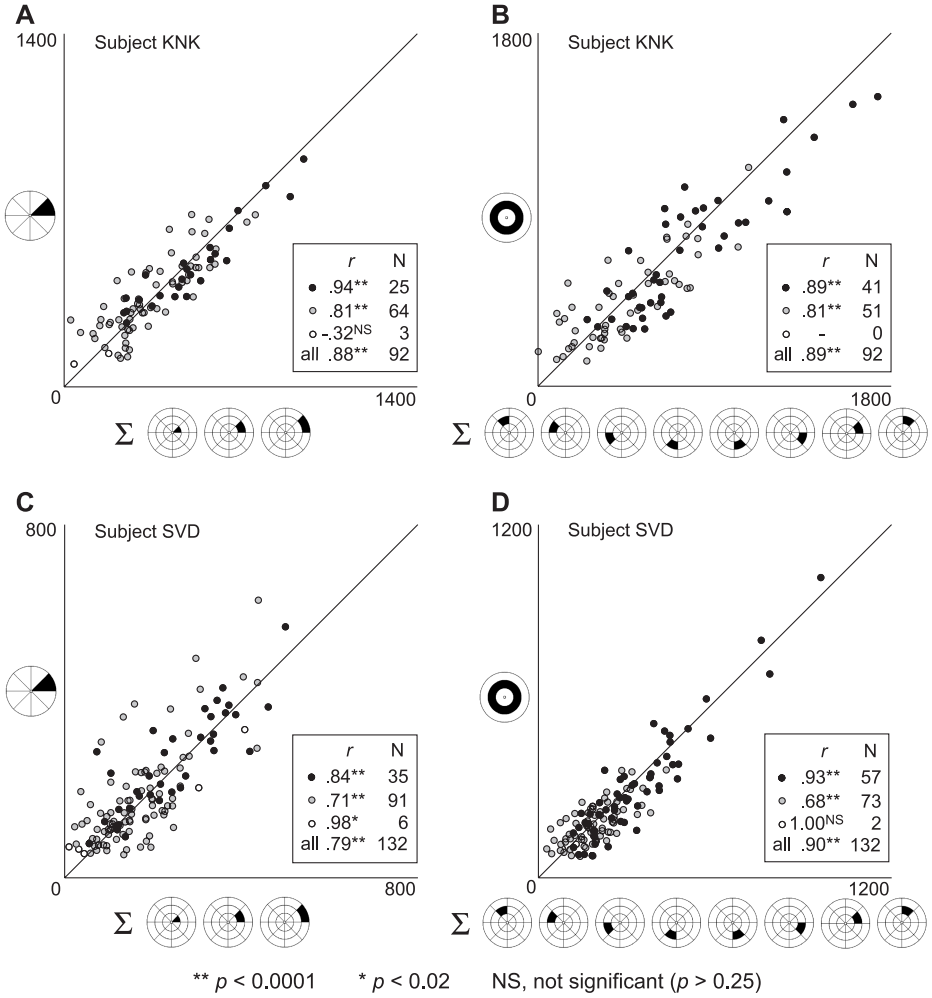

Fig. 5. Spatial summation predicts positive BOLD responses. (A) Each point represents BOLD responses of a single voxel. The *y*-axis gives the magnitude of the largest wedge response for each voxel. The *x*-axis gives the sum of the magnitudes of the responses to the component patches of the relevant wedge for each voxel. (For clarity the *y*-axis legend schematically portrays a single wedge, but responses to all wedges are included in the plot.) Units of response magnitudes are raw fMRI signal per unit stimulus. Dot shading represents the number of patches that evoked a significant positive response from each voxel. Black dots indicate voxels that responded significantly to at least two component patches. These critical voxels are likely to represent neural populations whose receptive fields span the border between patches. Gray dots indicate voxels with significant responses to exactly one component patch, and white dots indicate voxels with no significant response to any component patch. (B) Maximal responses to rings and sums of responses to component patches for the population of voxels shown in A. Dot shading same as A. (C) Data from subject SVD, same format as in panel A. (D) Data from subject SVD, same format as in panel B.

sensitive test should focus on the subset of voxels that give significant responses to two or more patches forming components of the tested wedge or ring. These voxels are likely to represent the borders between patches in retinotopic space (e.g., see Fig. 3C). If these voxels also show linear summation, then we can conclude that this is a general property. The relevant border voxels are shaded black in Fig. 5. It is clear that these points fall quite near the line of unity slope, the spread is small (see values of r, Fig. 5), and the outliers are distributed symmetrically. These data offer strong support for linearity by spatial summation.

Axis units are raw fMRI signal per unit stimulus ($h(\tau)$ from Eq. (2)). Raw fMRI signal per unit stimulus is analogous to neuronal spikes per unit stimulus, traditionally used for reverse correlation results in the electrophysiology literature. In the fMRI literature, it is untraditional: reverse correlation is an implementation of cross-correlation, and fMRI cross-correlation results are typically normalized to the unitless correlation coefficient (Bandettini et al., 1993). The correlation coefficient can be computed by replacing the factor σ_S^2 in Eq. (2) with $\sigma_R\sigma_S$, where σ_R is the standard deviation of the time series data. Here, we chose to retain raw fMRI signal per unit stimulus despite its arbitrary scale. If a suppressive or facilitatory spatial nonlinearity had been present, it could have been revealed by its effect on the variance of the time series data. Such an effect would have been obscured in the normalization to the correlation coefficient. Therefore, using the non-normalized units in the analysis increased sensitivity to potential nonlinearities.

Discussion

The experiment reported here clearly demonstrates that the BOLD response of single voxels in calcarine visual cortex is consistent with linearity by spatial summation. The positive BOLD responses to wedges and rings were well predicted by the sums of responses to the component patches of each wedge or ring. This was true both for voxels responding to only one patch within the relevant wedge or ring and for voxels responding to two or more component patches. Confirmation of linearity by spatial summation justifies the general application of spatially linear analyses to V1 BOLD data acquired using stimuli with different spatial characteristics and addresses previous concerns about such analyses (Smith et al., 2001).

Although the linearity we observe here is striking, it would not be appropriate to assume that every visual stimulus regime will result in spatially linear BOLD responses; some stimulus configurations may evoke spatially nonlinear BOLD responses in V1. Our experiments used a fairly coarse patch size, chosen to be consistent with the dimensions of wedges and rings used in typical retinotopic mapping experiments. It is possible that smaller stimuli might evoke spatially nonlinear responses. For example, nonlinear summation might occur if there are limits on the volume of blood that can be directed instantaneously to a portion of cortex. In this case, the BOLD response evoked by several stimuli presented simultaneously could be substantially less than would be predicted from the sum of BOLD responses to those same stimuli presented individually, reflecting saturation of blood delivery. Spatially nonlinear blood volume-related effects might also result from varying patterns of vasculature across cortex (Zheng et al., 1991).

Nonlinear spatial summation of BOLD might also occur when the underlying neural responses are spatially nonlinear. It has been suggested that nonlinear surround suppression of neural responses might lead to spatially nonlinear BOLD responses (Zenger-Landolt and Heeger, 2003), and nonlinear surround-suppressive effects have previously been reported in V1 BOLD signals (Press et al., 2001; Williams et al., 2003). However, the relatively coarse, high-contrast checkerboard patterns used in our experiments did not produce such an effect.

Finally, even if both BOLD and the underlying neural response are linear, experimental procedures may produce nonlinear artifacts. The sensitivity of our test of linearity by spatial summation was largely due to the use of M-sequences, which have very low stimulus cross- and auto-correlations (Sutter, 1992). Random binary sequences have much larger cross- and auto-correlations. (This is virtually always the case even when the least correlated sequence is chosen from a large set, unless the set is so large as to be impractical.) If we had used these stimuli instead, BOLD responses would have been contaminated by these stimulus correlations. These artifacts could have produced an apparent violation of linearity by spatial summation.

When designing our stimulus protocol we shifted the governing M-sequences by 30 s relative to one another, a period longer than the time constant of the hemodynamic response. If we had picked a shorter rotation period (e.g., 5 s, on the order of the hemodynamic time constant), then the responses to each stimulus would have been contaminated by substantial artifactual correlations with responses to other regions. Note that correlation artifacts such as this are unavoidable when spatially or temporally correlated stimuli are used. Data acquired with correlated stimuli should be corrected to remove correlation artifacts (Marmarelis and Marmarelis, 1978; Theunissen et al., 2001) when linearity is assumed.

Negative BOLD

A minority of the voxels shown in Fig. 5 (30 of 92 in subject KNK; 55 of 132 in subject SVD) gave a significant sustained negative BOLD response to at least one wedge, ring or patch. As reported in previous studies (Harel et al., 2002; Shmuel et al., 2002; Stefanovic et al., 2004), the time course of the sustained negative BOLD response follows that of the positive hemodynamic response, but the sustained negative BOLD response is inverted (Fig. 2C, blue trace). The sustained negative BOLD response is different in time course and amplitude from the "initial dip" observed using optical imaging (Frostig et al., 1990) and fMRI (Ernst and Hennig, 1994; Menon et al., 1993).

In the sustained negative BOLD response, the drop in the measured MR signal implies decreased homogeneity of the local magnetic field. Current proposals suggest that this phenomenon is due to a local increase in the concentration of deoxyhemoglobin, caused either by vascular interactions with active portions of cortex (Harel et al., 2002) or by the inhibition of neurons whose activity level influences vascular response. Inhibitory horizontal connections (or inhibitory connections between cortical areas) may mediate the sustained negative BOLD response (Shmuel et al., 2002), and performing a task known to induce neural inhibition has been shown to produce a sustained negative BOLD response (Stefanovic et al., 2004). Note that these potential signal sources are not mutually exclusive.

Spatial attention has been shown to increase V1-sustained negative BOLD response at unattended retinotopic locations (Smith et al., 2000; Slotnick et al., 2003; Tootell et al., 1998), although the physiological mechanism underlying this effect is not yet under-

stood. Our preliminary analyses suggest that the sustained negative BOLD response is poorly predicted by spatial summation (data not shown). However, our experiments did not manipulate attention systematically, so we cannot rule out the possibility that these effects reflect differential allocation of covert attention.

Response estimation procedure

Our study combines three basic methods: stimulus generation by M-sequences, reverse correlation analysis, and randomization statistics. When combined, these methods efficiently produce reliable and readily interpretable estimates of retinotopic responses. The use of M-sequences (Baseler et al., 1994; Slotnick et al., 1999) ensures that simultaneously presented stimuli contain no substantial temporal cross- or auto-correlations (Sutter, 1992). This minimizes temporal correlations and so should increase the effective spatial resolution of the resulting response sets.

Many fMRI studies use an indicator function, most often a prototypical hemodynamic response function, to facilitate regression of stimuli onto responses (Friston et al., 1995a, 1995b). These indicator functions have the virtue of making identification of some signals more robust and reliable. However, the shape of the optimal indicator function may vary between brain areas or across subjects (Handwerker et al., 2004), and an incorrectly chosen indicator function actually obscures signals. In contrast, the reverse correlation procedure used here provides independent estimates of the stimulus-response function at each time lag (Bandettini et al., 1993; Shmuel et al., 2002), thereby avoiding the problem of indicator function selection altogether.

There are several advantages to adding randomization-based statistical testing procedures to analyses of BOLD responses. Most importantly, randomization tests provide a direct estimate of the probability that the correlation between specific stimuli and BOLD responses could have occurred by chance alone. Because randomization tests are non-parametric statistical tests, they are valid even when the fMRI signals are non-Gaussian (Chen et al., 2003) or when the signal-to-noise ratio across voxels is not constant (Raz et al., 2003).

The experiment presented here focused on spatial responses, but similar procedures could be used to investigate other stimulus dimensions. In addition, our procedures allow simultaneous investigation of several stimulus classes, making effective use of valuable scan time. Our approach has already proven its value in the field of electrophysiology (Mazer et al., 2002; Theunissen et al., 2001).

Conclusion

The positive BOLD response in primary visual cortex is well predicted by linear spatial summation, at least at the spatial scale most relevant to typical retinotopic mapping experiments. However, nonlinear responses might occur at spatial scales not examined in this experiment. Subsequent experiments should employ smaller stimuli to determine whether BOLD response linearity breaks down at a finer spatial scale.

Acknowledgments

We thank Nicolas Cottaris for providing invaluable advice on M-sequence generation, Ben Inglis for assistance with and informative discussions about MRI data acquisition and Jamie Mazer for comments on the manuscript. We also thank David Heeger, who provided a critical insight into a potential connection between spatial attention and negative BOLD; his views have been incorporated into the manuscript.

References

Bandettini, P.A., Jesmanowicz, A., Wong, E.C., Hyde, J.S., 1993. Processing strategies for time-course data sets in functional MRI of the human brain. Magn. Reson. Med. 30, 161–173.

Baseler, H.A., Sutter, E.E., Klein, S.A., Carney, T., 1994. The topography of visual evoked response properties across the visual field. Electroencephalogr. Clin. Neurophysiol. 90, 65–81.

Birn, R.M., Saad, Z.S., Bandettini, P.A., 2001. Spatial heterogeneity of the nonlinear dynamics in the fMRI BOLD response. NeuroImage 14, 817–826.

Boynton, G.M., Engel, S.A., Glover, G.H., Heeger, D.J., 1996. Linear systems analysis of functional magnetic resonance imaging in human V1. J. Neurosci. 16, 4207–4221.

Buracas, G.T., Boynton, G.M., 2002. Efficient design of event-related fMRI experiments using M-sequences. NeuroImage 16, 801–813.

Chen, C.C., Tyler, C.W., Baseler, H.A., 2003. Statistical properties of BOLD magnetic resonance activity in the human brain. NeuroImage 20, 1096–1109.

Dale, A.M., Buckner, R.L., 1997. Selective averaging of rapidly presented individual trials using fMRI. Hum. Brain Mapp. 5, 329–340.

de Boer, E., Kuyper, P., 1968. Triggered correlation. IEEE Trans. Biomed. Eng. 15, 159–179.

DeYoe, E.A., Carman, G.J., Bandettini, P., Glickman, S., Wieser, J., Cox, R., Miller, D., Neitz, J., 1996. Mapping striate and extrastriate visual areas in human cerebral cortex. Proc. Natl. Acad. Sci. U. S. A. 93, 2382–2386.

Duvernoy, H.M., 1999. The Human Brain: Surface, Three-Dimensional Sectional Anatomy with MRI, and Blood Supply, 2nd ed. Springer-Verlag, Vienna.

Engel, S.A., Glover, G.H., Wandell, B.A., 1997. Retinotopic organization in human visual cortex and the spatial precision of functional MRI. Cereb. Cortex 7, 181–192.

Ernst, T., Hennig, J., 1994. Observation of a fast response in functional MR. Magn. Reson. Med. 32, 146–149.

Friston, K.J., Frith, C.D., Turner, R., Frackowiak, R.S., 1995a. Characterizing evoked hemodynamics with fMRI. NeuroImage 2, 157–165.

Friston, K.J., Poline, J.-B., Holmes, A., Frith, C.D., Frackowiak, R.S., 1995b. Statistical parametric maps in functional imaging: a general linear approach. Hum. Brain Mapp. 4, 140–151.

Friston, K.J., Josephs, O., Rees, G., Turner, R., 1998. Nonlinear event-related responses in fMRI. Magn. Reson. Med. 39, 41–52.

Frostig, R.D., Lieke, E.E., Ts'o, D.Y., Grinvald, A., 1990. Cortical functional architecture and local coupling between neuronal activity and the microcirculation revealed by in vivo high-resolution opical imaging of intrinsic signals. Proc. Natl. Acad. Sci. U. S. A. 87, 6082–6086.

Harel, N., Lee, S.P., Nagaoka, T., Kim, D.S., Kim, S.G., 2002. Abstract origin of negative blood oxygenation level-dependent fMRI signals. J. Cereb. Blood Flow Metab. 22, 908–917.

Handwerker, D.A., Ollinger, J.M., D'Esposito, M., 2004. Variation of BOLD hemodynamic responses across subjects and brain regions and their effects on statistical analyses. NeuroImage 21, 1639–1651.

Manly, B.F.J., 1991. Randomization and Monte-Carlo Methods in Biology. Chapman & Hall, New York, NY.

Marmarelis, P.Z., Marmarelis, V.Z., 1978. Analysis of Physiological Systems: The White Noise Approach. Plenum, New York, NY.

Mazer, J.A., Vinje, W.E., McDermott, J., Schiller, P.H., Gallant, J.L., 2002. Spatial frequency and orientation tuning dynamics in area V1. Proc. Natl. Acad. Sci. U. S. A. 99, 1645–1650.

Menon, R.S., Ogawa, S., Tank, D.W., Ugurbil, K., 1993. 4 Tesla gradient

recalled echo-time dependence of photic stimulation-induced signal changes in the human primary visual cortex. Magn. Reson. Med. 30, 380–386.

Press, W.A., Brewer, A.A., Dougherty, R.F., Wade, A.R., Wandell, B.A., 2001. Visual areas and spatial summation in human visual cortex. Vision Res. 41, 1321–1332.

Raz, J., Zheng, H., Ombao, H., Turetsky, B., 2003. Statistical tests for fMRI based on experimental randomization. NeuroImage 19, 226–232.

Sereno, M.I., Dale, A.M., Reppas, J.B., Kwong, K.K., Belliveau, J.W., Brady, T.J., Rosen, B.R., Tootell, R.B.H., 1995. Borders of multiple visual areas in humans revealed by functional magnetic resonance imaging. Science 268, 889–893.

Shmuel, A., Yacoub, E., Pfeuffer, J., Van de Moortele, P.-F., Adriany, G., Hu, X., Ugurbil, K., 2002. Sustained negative BOLD, blood flow and oxygen consumption response and its coupling to the positive response in the human brain. Neuron 36, 1195–1210.

Slotnick, S.D., Klein, S.A., Carney, T., Sutter, E., Dastmalchi, S., 1999. Using multi-stimulus VEP source localization to obtain a retinotopic map of human primary visual cortex. Clin. Neurophysiol. 110, 1793–1800.

Slotnick, S.D., Schwarzbach, J., Yantis, S., 2003. Attentional inhibition of visual processing in human striate and extrastriate cortex. NeuroImage 19, 1602–1611.

Smith, A.T., Singh, K.D., Greenlee, M.W., 2000. Attentional suppression of activity in the human visual cortex. Neuroreport 11, 271–277.

Smith, A.T., Singh, K.D., Williams, A.L., Greenlee, M.W., 2001. Estimating receptive field size from fMRI data in human striate and extrastriate visual cortex. Cereb. Cortex 11, 1182–1190.

Stefanovic, B., Warnking, J.M., Pike, G.B., 2004. Hemodynamic and metabolic responses to neuronal inhibition. NeuroImage 22, 771–778.

Sutter, E.E., 1992. Deterministic approach to nonlinear systems analysis. In: Pinter, R.B., Nabet, B. (Eds.), Nonlinear Vision: Determination of Neural Receptive Fields, Function and Networks. CRC Press, Boca Raton, pp. 171–220.

Theunissen, F.E., David, S.V., Singh, N.C., Hsu, A., Vinje, W.E., Gallant, J.L., 2001. Estimating spatio-temporal receptive fields of auditory and visual neurons from their responses to natural stimuli. Network 12, 289–316.

Tong, F., Engel, S.A., 2001. Interocular rivalry revealed in the human cortical blind-spot representation. Nature 411, 195–199.

Tootell, R.B.H., Hadjikhani, N., Hall, E.K., Marret, S., Vanduffel, W., Vaughan, J.T., Dale, A.M., 1998. The retinotopy of visual spatial attention. Neuron 21, 1409–1422.

Williams, A.L., Singh, K.D., Smith, A.T., 2003. Surround modulation measured with functional MRI in the human visual cortex. J. Neurophysiol. 89, 525–533.

Zenger-Landolt, B., Heeger, D.J., 2003. Response suppression in V1 agrees with psychophysics of surround masking. J. Neurosci. 23, 6884–6893.

Zheng, D., LaMantia, A.-S., Purves, D., 1991. Specialized vascularization of the primate visual cortex. J. Neurosci. 11, 2622–2629.